Macromolecules

COMMUNICATION TO THE EDITOR

pubs.acs.org/Macromolecules

Efficient Solar Cells from Semi-random P3HT Analogues Incorporating Diketopyrrolopyrrole

Petr P. Khlyabich, Beate Burkhart, Christi F. Ng, and Barry C. Thompson*

Department of Chemistry, Loker Hydrocarbon Research Institute, and Center for Energy Nanoscience, University of Southern California, Los Angeles, California 90089-1661, United States

Supporting Information

ABSTRACT: Three novel semi-random poly(3-hexylthiophene) (P3HT) based donor−acceptor copolymers containing 5−15% of the acceptor diketopyrrolopyrrole (DPP) were synthesized by Stille copolymerization and their optical, electrochemical, charge transport and photovoltaic properties were investigated. Poly(3-hexylthiophene-thiophene-diketopyrrolopyrrole) polymers with various percentages of DPP, represented as **P3HTT-DPP-5%**, **P3HTT-DPP-10%**, and **P3HTT-DPP-15%**, had high molecular weights (M_n 17 500−24 500 g/mol) and broad, intense absorption spectra, covering the spectral range from 350 nm up to 850 nm with absorption maxima at 685 and 703 nm for **P3HTT-DPP-10%** and **P3HTT-DPP-15%**. The low content of acceptor units allowed preservation of many important properties of P3HT, among which are semicrystallinity (as verified by GIXRD) and high hole mobilities ($\mu_h = (1-2.3) \times 10^{-4}$ cm^2/(V s)). Photovoltaic devices fabricated from P3HTT-DPP polymers blended with $PC_{61}BM$ showed higher short-circuit current densities (J_{sc}) of 9.57 − 13.87 mA/cm^2 compared to P3HT (9.49 mA/cm^2), leading to average power conversion efficiencies of 3.6−4.9%, which exceed the average value of 3.4% for P3HT under AM 1.5G illumination (100 mW/cm^2). External quantum efficiency (EQE) measurements revealed a strong photoresponse from the semirandom polymers up to 850 nm, with EQE values above 40% across the visible and into the near-infrared for **P3HTT-DPP-10%** and **P3HTT-DPP-15%**. These results indicate that semi-random P3HT analogues provide a simple and effective route toward polymers with a broad photocurrent response in bulk heterojunction solar cells.

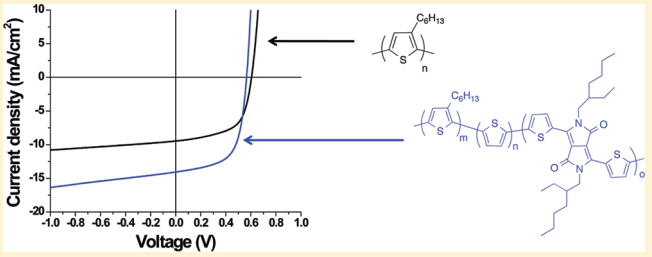

The ongoing development of an understanding of the operating principles of polymer-based bulk heterojunction (BHJ) photovoltaic devices[1−4] has given rise to increases in reported efficiencies, which now exceed 7%.[5−9] This rapid improvement in efficiency, along with the possibility for the economical fabrication of flexible, lightweight, and large area solar cells,[10] make organic photovoltaics a potential competitor to the crystalline silicon solar cells that currently dominate the market.[11] However, in order for polymer solar cells to become a viable technology, it is widely agreed that further increases in the efficiency (η) are needed (>10%).[12] The primary strategy toward this end has been the design of novel donor polymers, within the context of the highly successful and ubiquitous fullerene-based acceptors.[13,14] In this design process, there are numerous parameters of the polymeric donor that must be optimized. The first is the ability of the polymer to absorb light broadly across the solar spectrum with a high absorption coefficient (~10^5 cm^{-1}), as the short-circuit current density (J_{sc}) of the solar cell is proportional to the product of the spectral absorption breadth and absorption intensity of the active layer.[15] Second, the polymer must also have energy level offsets (with respect to the fullerene acceptor) positioned to provide sufficient driving force for charge generation and maximization of the open-circuit voltage (V_{oc}).[1] The polymer must also have a sufficiently high hole mobility to ensure effective charge extraction,[2] which is closely tied to the solid-state structure of the polymer and strongly affects the fill factor (FF).[16−18] Finally, any donor polymer must be capable of effective mixing with the fullerene acceptor in order to generate a bicontinuous morphology.[19,20]

For the first design parameter, broadening of the spectral absorption is usually targeted via the so-called donor−acceptor approach,[15,21] where electron-rich and electron-deficient units are polymerized in an alternating fashion along the polymer backbone, leading to a narrowing of the polymer bandgap (E_g). The desired consequence is the absorption of a larger fraction of solar photons and an increase in the J_{sc} and overall efficiency.[22] The main weakness of the alternating donor−acceptor strategy is the frequently observed shifting of the polymer absorption profile (relative to the pure donor homopolymer) to the long wavelength region as opposed to a true broadening across both the visible and near-infrared regions.[5,9,23−25] Decreasing the polymer absorption in the visible region of the solar spectrum can hinder the desired increase in the J_{sc} and ultimately the efficiency.

Recently, we reported a new class of donor−acceptor copolymers based on regioregular poly(3-hexylthiophene) (rr-P3HT or simply P3HT) called semi-random polymers, where only a small amount of acceptor units (10−17.5%) were introduced in a randomized fashion into the polymer backbone.[26] In this

Received: April 24, 2011
Revised: June 4, 2011
Published: June 14, 2011

Scheme 1. Synthesis and Structures of P3HTT-DPP-5%, P3HTT-DPP-10%, and P3HTT-DPP-15%.

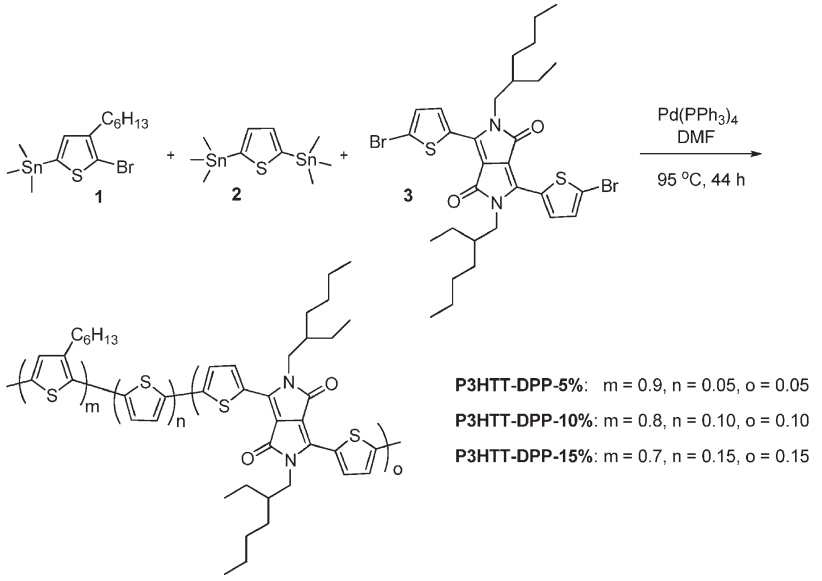

approach, monomer incorporation is controlled via a restricted linkage pattern of the donor and acceptor units, preventing the formation of acceptor-acceptor linkages as well as sterically unfavorable linkages, and preserving continuous segments of head-to-tail (regioregular) coupled 3-hexylthiophene. The randomized sequence distribution and nature of the donor−acceptor chromophores (based on the numerous possible chromophores defined by the effective conjugation length) generated broadly absorbing, multichromophoric polymers with intense absorption across the visible and up to 1000 nm. Importantly, the small percentage of the acceptor moieties preserved many of the important properties of P3HT that are conducive to high solar cell performance, among which are: semicrystallinity, high hole mobility and good miscibility with the fullerene acceptor $PC_{61}BM$. Polymer miscibility with the fullerene is important for minimizing the amount of fullerene required to generate a percolated network and maintaining the ability of the polymer to absorb a meaningful fraction of long wavelength light within the constraints of an active layer that cannot typically exceed a thickness of ~100 − 200 nm.[18,27−30] Solar cells, based on the previously synthesized semi-random polymers, showed moderate performance, but nonetheless indicated that semi-random polymers are interesting for further research as potentially attractive donor polymers for BHJ solar cells.

Here we report the first examples of semi-random P3HT analogues that give high efficiency in bulk heterojunction solar cells. In this study we have chosen diketopyrrolopyrrole (DPP)[31−35] as the acceptor unit and the effect of acceptor content on polymer properties and photovoltaic response is described. Three novel donor−acceptor polymers with different percentages of the DPP unit (5−15%) were synthesized. These polymers were fully characterized and used in BHJ solar cells with $PC_{61}BM$ as the acceptor, giving efficiencies reaching nearly 5%.

The synthesis of all three P3HTT-DPP polymers (P3HTT-DPP stands for poly(3-hexylthiophene−thiophene−diketopyrrolopyrrole)) were carried out in analogy to the previously reported semi-random P3HT analogues,[26] as illustrated in Scheme 1. Copolymerization of 2-bromo-5-trimethyltin-3-hexylthiophene (**1**) with 2,5-bis(trimethyltin) thiophene (**2**) and varying amounts of dibromo-bisthiophene-diketopyrrolopyrrole (**3**) in DMF at 95 °C with $Pd(PPh_3)_4$ as the catalyst, gave polymers with M_n 17 500−24 500 g/mol (see Supporting Information for polymer characterization data). Polymer structures were confirmed by ^1H NMR and it was found that polymer composition matched the monomer feed ratios, as we have previously observed with analogous semi-random polymers.[26] The resulting polymers are represented by the acronyms P3HTT-DPP-*X*%, where the percentage of DPP monomer is indicated, giving **P3HTT-DPP-5%**, **P3HTT-DPP-10%**, and **P3HTT-DPP-15%**. Synthetic procedures for the monomers, as well as detailed synthesis and purification procedures for the polymers are given in the Supporting Information.

The choice of the bisthiophene−diketopyrrolopyrrole (DPP) unit (monomer **3**) as the acceptor was influenced by the growing number of recent reports of high efficiency in BHJ solar cells with polymers[32−34] and small molecules[31] containing this unit, albeit with variable *N*-alkyl substitution. Introduction of the DPP unit into polymer backbones with different donor units[36−39] led to low optical band gaps (1.2−1.6 eV), photocurrent response up to 1100 nm,[40,41] J_{sc} of more than 10 mA/cm^2, and solar cell efficiencies of 4−5.5%.[32−34,38,42,43] The presence of one thiophene on each side of the DPP acceptor minimizes steric hindrance and induces planarity, which enhances chain packing and intermolecular $\pi-\pi$ interaction.[38,42,43] As a result, high hole mobilities are observed for DPP-containing polymers.[34] The DPP acceptor also influences the energy levels of the polymer, lowering the position of the HOMO and LUMO levels.[33,38] As a result, V_{oc} values in the range 0.8−0.9 V have been obtained.[32,38,39,44] These physical and electronic properties of DPP-based polymers, together with their observed thermal stability,[35,45] make DPP a very attractive unit for incorporation into semi-random copolymers.

The optical properties of the semi-random P3HTT-DPP polymers in *o*-dichlorobenzene (*o*-DCB) solutions and thin films were studied using UV−vis spectroscopy as shown in Figure 1. As a reference, data is shown for P3HT synthesized using analogous Stille polymerization conditions.[26] The introduction of DPP into the P3HT backbone is observed to significantly decrease the optical bandgap and lead to the formation of a

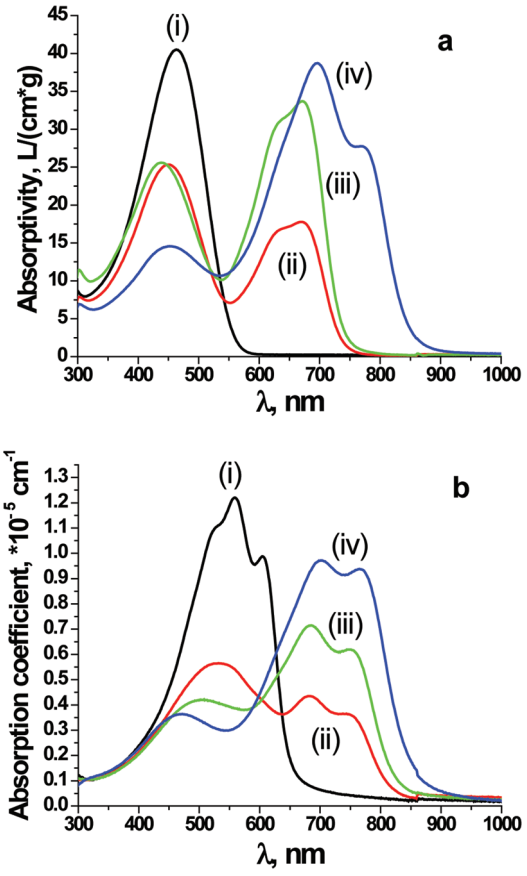

Figure 1. UV−vis absorption spectra of polymers in (a) solution (*o*-dichlorobenzene or *o*-DCB) and (b) thin film (spin-coated from *o*-DCB) where (i) is P3HT (annealed at 150 °C for 30 min for the thin films), (ii) is **P3HTT-DPP-5%** (thin film as-cast), (iii) is **P3HTT-DPP-10%** (thin film as-cast), and (iv) is **P3HTT-DPP-15%** (thin film as-cast).

distinct dual band absorption in solutions and thin films. This type of absorption profile is often ascribed to $\pi-\pi^*$ (short wavelength band) and ICT (intramolecular charge transfer) transitions (long wavelength band).[46,47] In the case of semi-random polymers, the dual band absorption could more specifically be assigned to $\pi-\pi^*$ transitions of segments in the randomized polymer that are thiophene-rich (short wavelength band) and ICT transitions in segments that are rich in donor−acceptor linkages (long wavelength band). This is especially evident in solution (Figure 1a) where pristine P3HT has a single absorption band with a peak at 463 nm and this absorption band is retained in all three P3HTT-DPP copolymers. With increasing content of DPP acceptor, the intensity and breadth of the long wavelength absorption band (donor−acceptor or ICT band) increases at the expense of the short wavelength band (thiophene $\pi-\pi^*$). More specifically, an increase of the DPP content leads to a red-shift and intensity increase of the ICT band, accompanied by a blue-shift and intensity decrease in the $\pi-\pi^*$ band, which is even more pronounced in thin films (Figure 1b).

Absorption coefficients in thin films of the ICT band of **P3HTT-DPP-10%** and especially **P3HTT-DPP-15%** are approaching 10^5 cm^{-1} and are comparable to the peak value of P3HT. Furthermore, the ICT peak positions of the P3HTT-DPP polymers are located close to the maximum of the photon flux from the sun, which is at 700 nm (1.8 eV).[15] It is notable that small red-shifts of the ICT peak positions for P3HTT-DPP polymers (10−15 nm), when going from solution to film, imply that already in solution the polymers adopt a planar conformation and upon film formation only a small reorganization and increase in packing between the polymer chains occurs (especially in the case of **P3HTT-DPP-15%**). This is in contrast to P3HT, which displays a 96 nm red-shift induced by significant ordering in the solid state. As a further point, thermal annealing is observed to enhance the thin film absorption of P3HT and affect the absorption profile.[48] The P3HTT-DPP thin film absorption spectra were collected with thin films spin-coated from *o*-DCB solution. It was observed that the films exhibited a rapid color change from dark green to gray-purple immediately after spin-coating was completed. Unlike P3HT, neither thermal annealing nor slow solvent evaporation had any effect on the absorption profiles. Overall, increasing the content of DPP in the polymer backbone gives rise to a relatively uniform absorption profile at low DPP content (5%), analogous to the multichromophoric description that we proposed for previously reported semi-random donor−acceptor copolymers.[26] However, as the DPP content increases (10 − 15%), the polymer absorption profile begins to converge toward that observed for perfectly alternating thiophene-DPP polymers, which contain significantly higher contents (50%) of DPP acceptor.[32−34,42,43]

Another interesting feature in the thin film absorption spectra is the presence of the vibronic features in the ICT band. The same vibrational shoulders were observed in the case of other DPP-based polymers and small molecules,[31,39] and were ascribed to the high degree of ordering and strong intermolecular ($\pi-\pi$) interactions.[33,49] To verify the formation of semicrystalline polymer thin films, grazing-incidence X-ray diffraction (GIXRD) was used (see Supporting Information for data). P3HTT-DPP polymers were spin-coated from *o*-DCB solutions under identical conditions used for the preparation of films for absorption spectra. **P3HTT-DPP-10%** was found to exhibit evidence of crystallinity in the as-cast films with an interchain distance (100) of 14.7 Å (for comparison, the P3HT interchain distance is 16.6 Å). In contrast, **P3HTT-DPP-5%** and **P3HTT-DPP-15%** show features indicative of crystalline order only upon annealing at 150 °C showing 16.0 and 16.2 Å interchain distances, respectively. Under the same thermal annealing condition, **P3HTT-DPP-10%** shows a more intense peak than that observed in the as-cast film and a larger interchain distance of 15.3 Å. The origin of the difference in initial ordering behavior of the as-cast films is not clear, although it could be partially attributed to the lower molecular weight and larger PDI of **P3HTT-DPP-5%** and **P3HTT-DPP-15%** (M_n = 19 000 g/mol, PDI = 2.8 and M_n = 17 570 g/mol, PDI = 2.9, respectively) compared to **P3HTT-DPP-10%** (M_n = 24 570 g/mol, PDI = 2.3). Slow solvent evaporation was observed to have no effect for any of the P3HTT-DPP polymers. However, all of the P3HTT-DPP polymers showed evidence of a semicrystalline structure.

The space-charge limited current (SCLC) method was employed to determine the hole mobilities of the P3HTT-DPP polymers. High hole mobilities in the range of (1−2.3) × 10^{-4} $cm^2/(V\,s)$ (Table 1) were obtained, which are close to that of P3HT and are attributed to the semicrystalline nature of the polymers revealed with the GIXRD. In contrast to GIXRD measurements, the maximum mobilities were obtained when a slow solvent evaporation technique was employed, where thin films were placed in a N_2 cabinet for 20 min before aluminum deposition.

The HOMO and LUMO energy levels for P3HT and the P3HTT-DPP polymers were measured by cyclic voltammetry

Table 1. Photovoltaic Properties of P3HT, P3HTT-DPP-5%, P3HTT-DPP-10%, and P3HTT-DPP-15% with $PC_{61}BM$ as an acceptor

polymer:$PC_{61}BM$ (ratio)	thickness (nm)[c]	SCLC hole mobility ($cm^2/(V\,s)$)[d]	J_{sc} (mA/cm^2)[e]	V_{oc} (V)	FF	η (%)
P3HT (1:1)[a]	95	2.3×10^{-4}	9.49	0.61	0.61	3.42
P3HTT-DPP-5% (1:1)[b]	74	1.1×10^{-4}	9.57	0.66	0.58	3.60
P3HTT-DPP-10% (1:1.3)[b]	71	2.3×10^{-4}	13.87	0.57	0.63	4.94
P3HTT-DPP-15% (1:2.6)[b]	75	1.3×10^{-4}	13.44	0.50	0.60	4.10

[a] Spin-coated from chlorobenzene (CB) and annealed at 150 °C for 30 min under N_2 after aluminum deposition. [b] Spin-coated from *o*-DCB and tested after spending 20 min in a N_2 cabinet before aluminum deposition. [c] Measured by X-ray reflectivity. [d] Measured for neat polymer films. [e] Mismatch corrected[54] (see Supporting Information).

(CV) with ferrocene as a reference, and converted to the vacuum scale using the approximation that the ferrocene redox couple is 5.1 eV relative to vacuum (see Supporting Information for the CV traces).[13,50,51] All P3HTT-DPP polymers, independent of the DPP content, showed a HOMO level of 5.2 eV, which is equivalent to that of P3HT. The measured position of the HOMO levels also indicates that the polymers should be resistive to air oxidation and thus facilitate device operational lifetime.[52,53]

The observed characteristics (high molecular weight, low bandgap, high absorption coefficient, high hole mobility) of the P3HTT-DPP polymers make them excellent candidates for photovoltaic devices. BHJ solar cells in a conventional device configuration of ITO/PEDOT:PSS/polymer:$PC_{61}BM$/Al were fabricated in air (see Supporting Information for the detailed device fabrication procedures). The optimized polymer:$PC_{61}BM$ weight ratios for **P3HTT-DPP-5%**, **P3HTT-DPP-10%**, **P3HTT-DPP-15%** were found to be 1:1, 1:1.3, and 1:2.6, respectively. Optimal processing conditions include slow solvent evaporation (solvent annealing) from the polymer:$PC_{61}BM$ composites for 20 min in a N_2 cabinet after spin-coating and prior to aluminum deposition, analogous to the conditions observed to give the highest mobilities for the polymers in the SCLC measurements. Interestingly the same solvent annealing process was not observed to give any changes in the GIXRD data or in the absorption spectra of the polymers. Shorter or longer solvent annealing times for the solar cells led to a decrease in J_{sc} and thermal annealing across a range of temperatures was also observed to decrease the performance of the solar cells. Table 1 lists the average values of η, V_{oc}, FF, and mismatch corrected[54] J_{sc} obtained under simulated AM 1.5G illumination (100 mW/cm^2) ($J-V$ curves are provided in the Supporting Information). For reference, the average efficiency measured here for P3HT:$PC_{61}BM$ solar cells is 3.42%. While this value is lower than reported champion level values of 4.5−5.0%, the difference is thought to primarily reflect the consequences of device fabrication and testing in air as opposed to an inert environment. High values of FF for all devices can be attributed to the high hole mobilities of the polymers, presumably leading to balanced charge transport in the devices and a reduction of recombination.[17,18,27] It is observed that the V_{oc} of the solar cells varies from 0.66 V with **P3HTT-DPP-5%** to 0.57 V with **P3HTT-DPP-10%**, to 0.50 V with the **P3HTT-DPP-15%**. The 160 mV range in the V_{oc} cannot be explained by differences between the HOMO of the donor and LUMO of the acceptor,[1] because the positions of the HOMO levels of the three P3HTT-DPP polymers are the same. We speculate that one possible explanation for the changes in the V_{oc} could be related to the increase of the degree of aggregation, when going from **P3HTT-DPP-5%** to **P3HTT-DPP-10%** to **P3HTT-DPP-15%**, supported by the observed decrease in the solubility of the polymers in *o*-DCB with increasing DPP content.[55] As such, the recombination rate could increase with increasing DPP content,[55−57] thus slowing down the kinetics of molecular electron transfer[58] and leading to the observed V_{oc} reduction. However, it should be noted that V_{oc} values observed for perfectly alternating DPP copolymers, which utilize thiophenes as the donor units were 0.63−0.68 V in $PC_{61}BM$ blends.[42,43] As such, the origins of this trend in the V_{oc} are under further investigation.

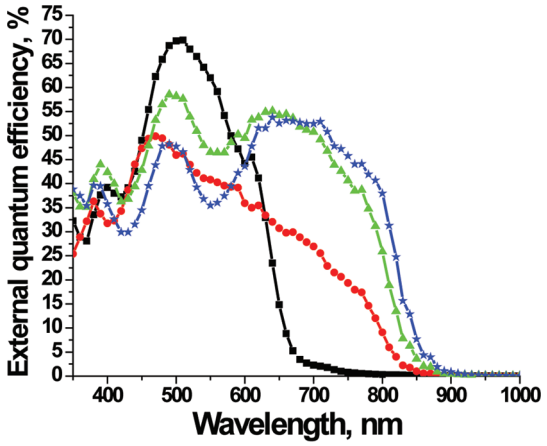

Figure 2. External quantum efficiency of the BHJ solar cells based on P3HT (black squares), **P3HTT-DPP-5%** (red circles), **P3HTT-DPP-10%** (green triangles) and **P3HTT-DPP-15%** (blue stars) with $PC_{61}BM$ as the acceptor, under optimized conditions for device fabrication.

A more easily explained trend is that of the J_{sc}, where the decrease of the polymer bandgap, relative to P3HT (J_{sc} = 9.49 mA/cm^2, mismatch correction M = 1.05), results in significant increases in the J_{sc}, giving 9.57 mA/cm^2 for **P3HTT-DPP-5%** (M = 0.87), 13.87 mA/cm^2 for **P3HTT-DPP-10%** (M = 0.76) and 13.44 mA/cm^2 for **P3HTT-DPP-15%** (M = 0.71). The highest observed J_{sc} value for **P3HTT-DPP-10%** can explained by the more balanced, intense absorption across the visible and near-infrared regions with respect to the other two DPP containing polymers and the smaller quantity of $PC_{61}BM$ needed to optimize device performance in comparison to **P3HTT-DPP-15%**.

The photocurrent response for all the optimized BHJ solar cells is shown in Figure 2. All devices showed strong photocurrent response in the range 350−850 nm, with EQE values of 41% and 46% at 750 nm for **P3HTT-DPP-10%** and **P3HTT-DPP-15%**, respectively. Photocurrent peaks around 400 nm are assigned to $PC_{61}BM$ light absorption, while photocurrent responses in the longer wavelength regions are attributed primarily to the polymers. The integrated photocurrents from the EQE measurement match within 5% to that of the mismatch corrected photocurrents measured under simulated AM 1.5G illumination (see

Supporting Information for mismatch corrected ($J_{sc,corr}$) and integrated ($J_{sc,EQE}$) photocurrents). A uniformly strong photocurrent response from the **P3HTT-DPP-10%** in the 350 − 850 nm range is explained by the favorable ratio of polymer to $PC_{61}BM$ of 1:1.3. In the case of perfectly alternating DPP-polymers, the best results were achieved at much higher polymer:fullerene ratios (1:2 and higher),[32−34,38,42,43] leading to a decrease in the uniformity of the photocurrent generation, especially in the near-infrared region, and hence smaller obtained J_{sc}.[38,42,43]

As further characterization of the BHJ solar cells, transmission electron microscopy (TEM) images (see Supporting Information) show the presence of uniform, bicontinuous thin films, with small length-scales of phase separation in $PC_{61}BM$ blends for all the P3HTT-DPP polymers. The observed morphologies are indistinguishable from optimized blends of P3HT and $PC_{61}BM$ and result in an apparent large interfacial area for efficient charge separation, which helps to explain the high attainable FFs and J_{sc} values for P3HT and P3HTT-DPP polymers. In general, the semi-random approach allows favorable morphology formation without application of any solvent additives[32,33] or thermal annealing[28] at a close to 1:1 polymer:fullerene ratio, when the acceptor content in the polymer backbone is low.

In summary, we have synthesized a family of novel semi-random P3HTT-DPP copolymers containing different contents (5−15%) of the DPP acceptor unit. These polymers combine broad absorption profiles, high absorption coefficients, high hole mobilities and semicrystalline structures similar to P3HT. In BHJ solar cells with $PC_{61}BM$, the polymers show effective film formation with optimized polymer:fullerene ratios that vary based on the content of DPP in the polymer backbone and efficiencies of nearly 5.0% are observed for **P3HTT-DPP-10%** at a 1:1.3 polymer:fullerene ratio. A broad photocurrent response, representative of the polymer absorption profile confirms that semi-random donor−acceptor copolymers are an effective platform for improving light harvesting in BHJ solar cells that further benefits from a simple and highly modular synthetic protocol. Ongoing studies are focused on elucidating the effect of acceptor−monomer content and identity on photovoltaic device parameters.

■ ASSOCIATED CONTENT

Supporting Information. Synthetic and solar cell fabrication and measurement procedures and NMR, CV, GIXRD, TEM, $J-V$, and mobility data. This material is available free of charge via the Internet at http://pubs.acs.org.

■ AUTHOR INFORMATION

Corresponding Author
*E-mail: barrycth@usc.edu.

■ ACKNOWLEDGMENT

This material is based upon work supported as part of the Center for Energy Nanoscience, an Energy Frontier Research Center funded by the U.S. Department of Energy, Office of Science, Office of Basic Energy Sciences under Award Number DE-SC0001013. Acknowledgement is made to the donors of the Petroleum Research Fund, administered by the American Chemical Society, for support under Award Number 49734-DNI10 for support of B.B. Support is acknowledged for C.F.N. from the USC Wise (Women in Science and Engineering) College Undergraduate Research Fellowship (Spring 2011) and the USC Provost's Undergraduate Research Fellowship (Summer 2010). We would also like to thank Prof. Mark E. Thompson for use of a potentiostat and setup for measuring EQE.

■ REFERENCES

(1) Thompson, B. C.; Khlyabich, P. P.; Burkhart, B.; Aviles, A. E.; Rudenko, A.; Shultz, G. V.; Ng, C. F.; Mangubat, L. B. *Green* **2011**, *1*, 29–54.
(2) Clarke, T. M.; Durrant, J. R. *Chem. Rev.* **2010**, *110*, 6736–6767.
(3) Deibel, C.; Dyakonov, V. *Rep. Prog. Phys.* **2010**, *73*, 096401.
(4) Kippelen, B.; Brédas, J.-L. *Energy Environ. Sci.* **2009**, *2*, 251–261.
(5) Chen, H.-Y.; Hou, J.; Zhang, S.; Liang, Y.; Yang, G.; Yang, Y.; Yu, L.; Wu, Y.; Li, G. *Nat. Photonics* **2009**, *3*, 649–653.
(6) Liang, Y.; Xu, Z.; Xia, J.; Tsai, S.-T.; Wu, Y.; Li, G.; Ray, C.; Yu, L. *Adv. Mater.* **2010**, *22*, E135–E138.
(7) Zhou, H.; Yang, L.; Stuart, A. C.; Price, S. C.; Liu, S.; You, W. *Angew. Chem., Int. Ed.* **2011**, *50*, 2995–2998.
(8) Price, S. C.; Stuart, A. C.; Yang, L.; Zhou, H.; You, W. *J. Am. Chem. Soc.* **2011**, *133*, 4625–4631.
(9) Chu, T.-Y.; Lu, J.; Beaupré, S.; Zhang, Y.; Pouliot, J.-R.; Wakim, S.; Zhou, J.; Leclerc, M.; Li, Z.; Ding, J.; Tao, Y. *J. Am. Chem. Soc.* **2011**, *133*, 4250–4253.
(10) Krebs, F. C. *Sol. Energy Mater. Sol. Cells* **2009**, *93*, 394–412.
(11) Avrutin, V.; Izyumskaya, N.; Morkoç, H. *Superlattices Microstruct.* **2011**, *49*, 337–364.
(12) Brabec, C. J.; Gowrisanker, S.; Halls, J. J. M.; Laird, D.; Jia, S.; Williams, S. P. *Adv. Mater.* **2010**, *22*, 3839–3856.
(13) Thompson, B. C.; Fréchet, J. M. J. *Angew. Chem., Int. Ed.* **2008**, *47*, 58–77.
(14) Dennler, G.; Scharber, M. C.; Brabec, C. J. *Adv. Mater.* **2009**, *21*, 1323–1338.
(15) Bundgaard, E.; Krebs, F. *Sol. Energy Mater. Sol. Cells* **2007**, *91*, 954–985.
(16) Mihailetchi, V.; Wildeman, J.; Blom, P. *Phys. Rev. Lett.* **2005**, *94*, 126602.
(17) Koster, L. J. A.; Mihailetchi, V. D.; Blom, P. W. M. *Appl. Phys. Lett.* **2006**, *88*, 052104.
(18) Kotlarski, J. D.; Moet, D. J. D.; Blom, P. W. M. *J. Polym. Sci., Part B: Polym. Phys.* **2011**, *49*, 708–711.
(19) van Bavel, S.; Veenstra, S.; Loos, J. *Macromol. Rapid Commun.* **2010**, *31*, 1835–1845.
(20) Moulé, A. J.; Meerholz, K. *Adv. Funct. Mater.* **2009**, *19*, 3028–3036.
(21) Kroon, R.; Lenes, M.; Hummelen, J.; Blom, P.; de Boer, B. *Polym. Rev.* **2008**, *48*, 531–582.
(22) Peet, J.; Kim, J. Y.; Coates, N. E.; Ma, W. L.; Moses, D.; Heeger, A. J.; Bazan, G. C. *Nat. Mater.* **2007**, *6*, 497–500.
(23) Liang, Y.; Feng, D.; Wu, Y.; Tsai, S.-T.; Li, G.; Ray, C.; Yu, L. *J. Am. Chem. Soc.* **2009**, *131*, 7792–7799.
(24) Hou, J.; Chen, H.-Y.; Zhang, S.; Chen, R. I.; Yang, Y.; Wu, Y.; Li, G. *J. Am. Chem. Soc.* **2009**, *131*, 15586–15587.
(25) Allard, N.; Aich, R. B.; Gendron, D.; Boudreault, P.-L. T.; Tessier, C.; Alem, S.; Tse, S.-C.; Tao, Y.; Leclerc, M. *Macromolecules* **2010**, *43*, 2328–2333.
(26) Burkhart, B.; Khlyabich, P. P.; Cakir Canak, T.; LaJoie, T. W.; Thompson, B. C. *Macromolecules* **2011**, *44*, 1242–1246.
(27) Kim, M.-S.; Kim, B.-G.; Kim, J. *ACS Appl. Mater. Interfaces* **2009**, *1*, 1264–1269.
(28) van Bavel, S.; Sourty, E.; de With, G.; Frolic, K.; Loos, J. *Macromolecules* **2009**, *42*, 7396–7403.
(29) Lenes, M.; Koster, L. J. A.; Mihailetchi, V. D.; Blom, P. W. M. *Appl. Phys. Lett.* **2006**, *88*, 243502.
(30) Min Nam, Y.; Huh, J.; Ho, Jo, W. *Sol. Energy Mater. Sol. Cells* **2010**, *94*, 1118–1124.

(31) Walker, B.; Tamayo, A. B.; Dang, X.-D.; Zalar, P.; Seo, J. H.; Garcia, A.; Tantiwiwat, M.; Nguyen, T.-Q. *Adv. Funct. Mater.* **2009**, *19*, 3063–3069.
(32) Bijleveld, J. C.; Gevaerts, V. S.; Di Nuzzo, D.; Turbiez, M.; Mathijssen, S. G. J.; de Leeuw, D. M.; Wienk, M. M.; Janssen, R. A. J. *Adv. Mater.* **2010**, *22*, E242–E246.
(33) Woo, C. H.; Beaujuge, P. M.; Holcombe, T. W.; Lee, O. P.; Fréchet, J. M. J. *J. Am. Chem. Soc.* **2010**, *132*, 15547–15549.
(34) Bronstein, H.; Chen, Z.; Ashraf, R. S.; Zhang, W.; Du, J.; Durrant, J. R.; Shakya Tuladhar, P.; Song, K.; Watkins, S. E.; Geerts, Y.; Wienk, M. M.; Janssen, R. A. J.; Anthopoulos, T.; Sirringhaus, H.; Heeney, M.; McCulloch, I. *J. Am. Chem. Soc.* **2011**, *133*, 3272–3275.
(35) Tieke, B.; Rabindranath, A. R.; Zhang, K.; Zhu, Y. *Beilstein J. Org. Chem.* **2010**, *6*, 830–845.
(36) Zou, Y.; Gendron, D.; Neagu-Plesu, R.; Leclerc, M. *Macromolecules* **2009**, *42*, 6361–6365.
(37) Bijleveld, J. C.; Karsten, B. P.; Mathijssen, S. G. J.; Wienk, M. M.; de Leeuw, D. M.; Janssen, R. A. J. *J. Mater. Chem.* **2011**, *21*, 1600–1606.
(38) Huo, L.; Hou, J.; Chen, H.-Y.; Zhang, S.; Jiang, Y.; Chen, T. L.; Yang, Y. *Macromolecules* **2009**, *42*, 6564–6571.
(39) Zoombelt, A. P.; Mathijssen, S. G. J.; Turbiez, M. G. R.; Wienk, M. M.; Janssen, R. A. J. *J. Mater. Chem.* **2010**, *20*, 2240–2246.
(40) Zhou, E.; Yamakawa, S.; Tajima, K.; Yang, C.; Hashimoto, K. *Chem. Mater.* **2009**, *21*, 4055–4061.
(41) Zhou, E.; Wei, Q.; Yamakawa, S.; Zhang, Y.; Tajima, K.; Yang, C.; Hashimoto, K. *Macromolecules* **2010**, *43*, 821–826.
(42) Wienk, M. M.; Turbiez, M.; Gilot, J.; Janssen, R. A. J. *Adv. Mater.* **2008**, *20*, 2556–2560.
(43) Bijleveld, J. C.; Zoombelt, A. P.; Mathijssen, S. G. J.; Wienk, M. M.; Turbiez, M.; de Leeuw, D. M.; Janssen, R. A. J. *J. Am. Chem. Soc.* **2009**, *131*, 16616–16617.
(44) Badrou Aïch, R.; Zou, Y.; Leclerc, M.; Tao, Y. *Org. Electron.* **2010**, *11*, 1053–1058.
(45) Tamayo, A. B.; Walker, B.; Nguyen, T.-Q. *J. Phys. Chem. C* **2008**, *112*, 11545–11551.
(46) Zhu, Y.; Champion, R. D.; Jenekhe, S. A. *Macromolecules* **2006**, *39*, 8712–8719.
(47) Beaujuge, P. M.; Amb, C. M.; Reynolds, J. R. *Acc. Chem. Res.* **2010**, *43*, 1396–1407.
(48) Kim, Y.; Cook, S.; Tuladhar, S. M.; Choulis, S. A.; Nelson, J.; Durrant, J. R.; Bradley, D. D. C.; Giles, M.; McCulloch, I.; Ha, C.-S.; Ree, M. *Nat. Mater.* **2006**, *5*, 197–203.
(49) Jo, J.; Gendron, D.; Najari, A.; Moon, J. S.; Cho, S.; Leclerc, M.; Heeger, A. J. *Appl. Phys. Lett.* **2010**, *97*, 203303.
(50) Thompson, B. C.; Kim, Y.-G.; McCarley, T. D.; Reynolds, J. R. *J. Am. Chem. Soc.* **2006**, *128*, 12714–12725.
(51) Cardona, C. M.; Li, W.; Kaifer, A. E.; Stockdale, D.; Bazan, G. C. *Adv. Mater.* **2011**, *23*, 2367–2371.
(52) Thompson, B. C.; Kim, Y.-G.; Reynolds, J. R. *Macromolecules* **2005**, *38*, 5359–5362.
(53) Jørgensen, M.; Norrman, K.; Krebs, F. C. *Sol. Energy Mater. Sol. Cells* **2008**, *92*, 686–714.
(54) Shrotriya, V.; Li, G.; Yao, Y.; Moriarty, T.; Emery, K.; Yang, Y. *Adv. Funct. Mater.* **2006**, *16*, 2016–2023.
(55) Kim, B.-G.; Jeong, E. J.; Park, H. J.; Bilby, D.; Guo, L. J.; Kim, J. *ACS Appl. Mater. Interfaces* **2011**, *3*, 674–680.
(56) Maurano, A.; Hamilton, R.; Shuttle, C. G.; Ballantyne, A. M.; Nelson, J.; O'Regan, B.; Zhang, W.; McCulloch, I.; Azimi, H.; Morana, M.; Brabec, C. J.; Durrant, J. R. *Adv. Mater.* **2010**, *22*, 4987–4992.
(57) Deibel, C.; Strobel, T.; Dyakonov, V. *Adv. Mater.* **2010**, *22*, 4097–4111.
(58) Schlenker, C. W.; Thompson, M. E. *Chem. Commun.* **2011**, *47*, 3702–3716.